

## Geometric Scaling in Inclusive $eA$ Reactions and Nonlinear Perturbative QCD

A. Freund,<sup>1</sup> K. Rummukainen,<sup>2</sup> H. Weigert,<sup>1</sup> and A. Schäfer<sup>1</sup>

<sup>1</sup>*Institut für Theoretische Physik, Universität Regensburg, D-93040 Regensburg, Germany*

<sup>2</sup>*NORDITA, DK-2100 Copenhagen, Denmark and Department of Physics, University of Helsinki, P.O. Box 64, FIN-00014, Helsinki, Finland*

(Received 6 December 2002; published 3 June 2003)

We report on geometric scaling in inclusive  $eA$  scattering data from the NMC and E665 experiments. This scaling and nuclear shadowing follows the pattern expected from nonlinear perturbative QCD for zero impact parameter at sufficiently small  $x_{bj}$  and is compatible with geometric scaling in  $ep$ .

DOI: 10.1103/PhysRevLett.90.222002

PACS numbers: 13.60.Hb, 12.38.Cy

*Introduction.*—Perturbative QCD (pQCD), in particular, where based on factorization theorems for high energy processes, has been very successful in describing data from high energy experiments. However, perturbative evolution has almost always been *linear* in the parton densities, which was, and very often still is, quite sufficient to describe high energy scattering.

There are, however, situations where this is bound to fail. Among those are high energy scatterings at energies large enough to create a gluon medium in which multi-gluon correlations can no longer be neglected. This was first discussed in the context of deep inelastic scattering of electrons off (large) nuclei, where both the large number of nucleons and the high energy lead to an increase in the number of gluons involved in the scattering [1–10]. In this regime nonlinear effects, leading to a taming or saturation/unitarization of  $F_2^A$ , should be included.

In the guise of a very successful phenomenological fit [11], this idea has even been applied at the DESY  $ep$  collider HERA (Hadron Electron Ring Accelerator) with its strong and, if untamed, unitarity violating rise of the proton structure function  $F_2^p(x_{bj}, Q^2)$  with decreasing  $x_{bj}$  [12,13]. This has led to the observation of “geometric scaling” satisfied by HERA data in the small  $x_{bj}$  region [14]. Our main focus is to extend this geometric scaling idea to nuclei and to check if it is already confirmed by available  $eA$  data.

The question of the onset of this saturation/unitarization in inclusive QCD observables with increasing energy (decreasing  $x_{bj}$ ), in particular, in the proton structure function  $F_2^p(x_{bj}, Q^2)$ , has been the subject of active discussions for many years (see a detailed discussion of this subject in [8,11,14] and references therein). Phenomenologically, the key feature at small  $x_{bj}$  is the simple structure of the total  $\gamma^*p$  cross section or  $F_2^{p,A}$  that arises directly from the underlying physics picture. Viewed in the infinite momentum frame of the target, the virtual photon splits into a  $q\bar{q}$  color dipole (treated as eikonalized Wilson lines) with a distribution characterized by  $Q^2$ . This dipole then punches through and interacts with the target, which it sees as a pancake of infinitesimal

longitudinal thickness. Consequently, the cross section appears as a convolution of the square of a photon wave function, which gives the probability to create the  $q\bar{q}$  pair, and a dipole cross section, which contains all the information about the target and the strong interaction physics.

The latter carries  $x_{bj}$  dependence which arises from gluonic fluctuations which induce an increase in the number of gluons. From this point of view, the target will display a growing density of gluons per transverse area (integrated over the longitudinal extent of the target) that drives the system into a saturation regime. The corresponding formula for the total cross section in  $\gamma^*p$  is then

$$\sigma_{\text{tot}}(x_{bj}, Q^2) = \int d^2z \int_0^1 d\alpha |\psi_{\gamma^*}(\alpha, z^2, Q^2)|^2 \times \sigma_{\text{dipole}}(x_{bj}, z^2), \quad (1)$$

where  $\alpha$  is the longitudinal momentum fraction of the  $q$  or  $\bar{q}$  and  $z$  is their relative transverse separation. Note that the  $Q^2$  and  $x_{bj}$  dependence is clearly separated into wave function and dipole cross section. This reflects the natural distinction between the transverse and longitudinal directions seen at high energies.  $Q^2$  sets the scale for transverse resolution, but longitudinal information about the target is subsumed in the  $x_{bj}$  dependence of the dipole cross section. The idea is that the dipole cross section depends on  $x_{bj}$  only via a scale  $Q_s(x_{bj})$  as  $\sigma_{\text{dipole}}(x_{bj}, z^2) = \sigma_{\text{dipole}}[z^2 Q_s^2(x_{bj})]$ .  $Q_s$  is the saturation scale, i.e., the scale below which the gluonic content of the target becomes “black” or  $\sigma_{\text{dipole}}$  reaches its large size asymptotics.

Together with Eq. (1) this implies that  $\sigma_{\text{tot}}$  and hence  $F_2^p$  scales according to

$$\sigma_{\text{tot}}(x_{bj}, Q^2) = \sigma_{\text{tot}}\left(x_0, \frac{Q^2}{Q_s^2(x_{bj})} Q_0^2\right). \quad (2)$$

This phenomenon is called geometric scaling and, as already mentioned, was first observed to be present in HERA data [14]. The fit used in [11,14] assumes an “eikonal” shape for  $\sigma_{\text{dipole}}$  that saturates for large dipoles. As  $x_{bj}$  decreases this saturation affects smaller and

smaller distances, inducing  $Q_s$  to grow, a fact which was parametrized by

$$Q_s(x_{bj}) := \left(\frac{x_0}{x_{bj}}\right)^\lambda Q_0. \quad (3)$$

A theoretical basis for such saturation/unitarization features, with a scaling behavior as in Eq. (2), together with precisely the functional dependence of  $Q_s$  as in Eq. (3) exists only at zero impact parameter  $b$ . It lies in nonlinear evolution equations that predict the small  $x_{bj}$  dependence from first principles.

The most promising approach to properly include saturation/unitarization is the Jalilian-Marian–Iancu–McLerran–Weigert–Leonidov–Kovner (JIMWLK) equation [5,6,8–10] the most compact form of which was derived in [8]. This equation resums the leading  $\ln(1/x_{bj})$  terms in *all*  $n$ -point correlation functions of the participating fields, not just the leading correlators as in  $k_\perp$  factorization. This leads to a nonlinear renormalization group equation for the generating functional for these  $n$ -point correlators which slows down the rapid growth of structure functions at small  $x_{bj}$  while at the same time preventing the system from drifting into the infrared where the densities are large, i.e., at  $b = 0$ . There, one has a self-consistent perturbative treatment not yet available at large  $b$ . At large  $N_c$  one recovers the Balitsky-Kovchegov and at small densities the Balitskii-Fadin-Kuraev-Lipatov (BFKL) equation [8,15]. We thus learn to interpret the loss of infrared safety in BFKL at  $b = 0$  as being due to the absence of any nonlinear corrections and the predicted too rapid a growth in  $F_2^p(x_{bj}, Q^2)$  as signals of BFKL having exceeded its range of validity. The full content of the JIMWLK equation can be accessed numerically: being a functional Fokker-Plank equation it can be rewritten in Langevin form, which then can be solved using lattice methods [16]. This will yield the  $x_{bj}$  dependence of  $\sigma_{\text{dipole}}$  and the evolution “rate”  $\lambda$  of Eq. (3).

Of particular interest to us in this context is the fact that the evolution equation is *target independent*. Target dependence arises only from the initial conditions for the  $x_{bj}$  dependence of the dipole cross section (related to the initial distribution of gluons in the transverse plane), which, in particular, are  $A$  dependent. These facts allow us to compare  $ep$  and  $eA$  scattering and investigate whether one of the basic predictions of this approach, geometric scaling, can also be found in inclusive  $eA$  processes.

*Geometric scaling and nuclear shadowing within non-linear pQCD.*—Before talking about geometric scaling in  $eA$  scattering, one should address nuclear shadowing or the suppression of  $\frac{1}{A}F_2^A$  to  $F_2^p$  at small  $x_{bj}$ . If this is at all possible it increases our phenomenological leverage considerably by allowing us to compare experiments with different  $A$  and  $x_{bj}$  directly. This is of particular impor-

tance as the available  $eA$  data do not offer any lever arm in  $x_{bj}$  for a given  $Q^2$  or vice versa.

In fact, the leading effect of nuclear shadowing can be easily incorporated in this approach by realizing that the change in transverse size simply changes the overall normalization of  $\sigma_{\text{dipole}}$ , while the change in longitudinal extent can be incorporated by increasing our initial  $Q_s$  by a factor of  $A^\delta$ . In the simplest case, assuming the distribution of spectator partons in the target to be homogeneous,  $\delta = 1/3$ . Equation (2) for  $F_2 \sim \sigma \cdot Q^2$  then turns into

$$\left(\frac{x_{bj}}{x_0}\right)^{2\lambda} \frac{F_2^A(x_{bj}, Q^2)}{A^{2/3+1/3}} = F_2^p \left[ x_0, \left(\frac{x_{bj}}{x_0}\right)^{2\lambda} \frac{Q^2}{A^{1/3}} \right]. \quad (4)$$

Note that  $0 \leq x_{bj} \leq A$  since  $x_{bj}$  is given per nucleon. The power  $2/3$  in the overall  $A$  dependence stems from a simple geometric factor, the area of the target, in the impact parameter integral in  $\sigma_{\text{dipole}}$ . Thus we have an unambiguous prediction for  $\frac{1}{A}F_2^A$  which states that not only can the observed nuclear shadowing in the  $eA$  data be explained by a simple rescaling of the variable  $Q^2$  with  $A^{1/3}$ , but also that all  $\frac{1}{A}F_2^A$  data, plotted vs  $\tau = \left(\frac{x_{bj}}{x_0}\right)^{2\lambda} \frac{Q^2}{A^{1/3}}$ , should lie on the same curve as the data for  $F_2^p$ . Hence, this approach also predicts geometric scaling in inclusive  $eA$  scattering analogous to the one observed in  $ep$  scattering.

*Geometric scaling in  $\frac{1}{A}F_2^A$ .*—Note that Eq. (4) is strictly true only at  $b = 0$  in the asymptotic region of small  $x_{bj}$ , large  $Q^2$ , and large nuclei. Therefore, we expect that there might be nonperturbative corrections which can spoil the form of Eq. (4) and consequently we perform a fit to the combined nuclear data with the following form:

$$\left(\frac{x_{bj}}{x_0}\right)^{2\lambda} \frac{1}{A^\gamma} \frac{1}{A} F_2^A(x_{bj}, Q^2) = F_2^p \left[ x_0, \left(\frac{x_{bj}}{x_0}\right)^{2\lambda} \frac{Q^2}{A^\delta} \right], \quad (5)$$

where  $\gamma$  and  $\delta$  are the fit parameters, which ideally would be 0 and  $1/3$ , respectively.

The starting point of our analysis is the published New Muon Collaboration (NMC) [17] and E665 [18,19] data for the ratios of nuclear to deuterium structure functions  $2F_2^A/A F_2^D$ . In Fig. 1 we show the ratios as functions of  $x$ . From these ratios we obtain the nuclear structure functions  $F_2^A$  as follows: we first note that NMC data show the deuterium to proton structure function ratio being  $F_2^D/2F_2^p = 1$  to better than 95% accuracy in the dynamical range of interest ( $x_{bj} < 0.1$ ) [17], which is well within the error margins of the nuclear  $F_2$  measurements. Thus, we convert  $F_2^A/F_2^D$  to structure functions  $F_2^A$  by multiplying the ratios by  $F_2^p$ , using the geometric scaling ansatz to extrapolate  $F_2^p$  to the appropriate values of  $x_{bj}$  and  $Q^2$ . Note that both HERA and NMC  $F_2^p$  scale only below  $x < 10^{-2}$  with the latter covering a much smaller  $Q^2$  and hence  $\tau$  range. We thus use the extracted HERA scaling curve for  $F_2^p$  to obtain the NMC  $F_2^A$ . We sketch the kinematic ranges in Fig. 2.

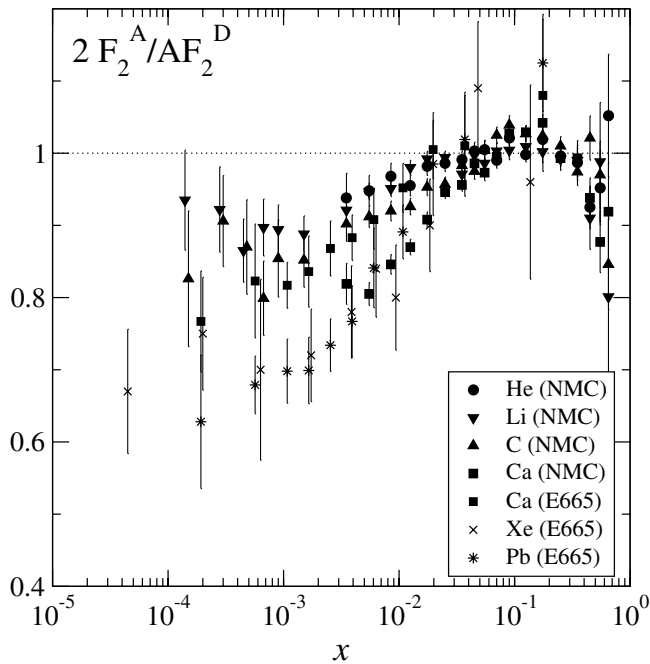


FIG. 1. Ratio of  $2F_2^A/AF_2^D$  vs  $\tau$  for NMC and E665. Note the increasing steepness with  $A$  within the NMC and E665 datasets, respectively.

Now we are ready to use Eq. (5) to compare nuclear and proton structure functions. In Fig. 3 the rescaled  $F_2^A$  is seen to fall on top of the dashed line representing the geometric scaling fit to the HERA  $F_2^p$ . For comparison we also show the quality of the scaling fit within the HERA data, offset by a factor of 5. We also note that the recent HERMES data on  $F_2^A$  [20] is in good agreement with this

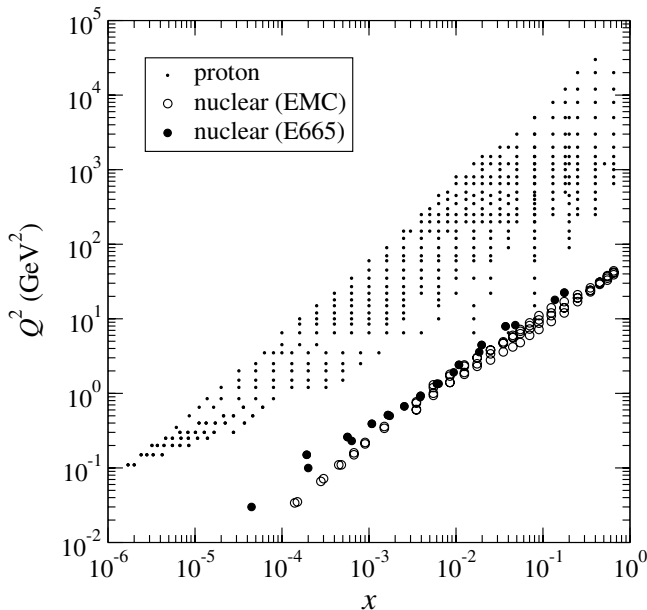


FIG. 2. Comparative phase space of HERA, NMC, and E665.

scaling behavior, however, clustered around  $0.8 \leq \tau \leq 10^2$ . Because of this small lever arm, the HERMES data alone have little restrictive power on  $\gamma$  and  $\delta$ . 95% of the HERMES data points have a scaled ratio  $F_2^A/AF_2^p$  between 0.9 and 1.1 when included into Fig. 4. We have chosen not to display this large number of additional data points for reasons of clarity.

The best fit to the combined nuclear data is achieved for  $\gamma = 0.09$  and  $\delta = 1/4$  which are close to but not quite the asymptotic values the nonlinear pQCD approach predicts. The remaining parameter  $\lambda \sim 0.18$  in Eq. (5) is already determined from the geometric scaling fit to the HERA data. With this value for  $\lambda$ , the saturation scale at the upper end of the HERA shadowing region at  $x_0 = 10^{-2}$  comes out to be marginally “perturbative,”  $Q_s^2 = 1 \text{ GeV}^2$ . Note that the region of phase space in which geometric scaling is present will, in general, depend on  $x_{bj}$ ,  $Q^2$ , and  $A$ . Only within this region a lower value of  $Q^2$  can be compensated by an appropriately larger value of  $A$ . We found that the NMC calcium data allows a smaller value of  $\gamma$  and, more importantly, a value of  $\delta = 1/3$  if the data on lighter nuclei is left out. This can be seen best in a log-linear plot of the scaled  $F_2$  ratios shown in Fig. 4, where the plateau from  $\tau = 0.1$  to  $\tau = 10$  shows good overall scaling behavior.  $\delta = 1/3$  would lift the NMC Ca data fully up to 1. This seems to indicate that the Ca nucleus is large enough for the basic assumptions of the nonlinear pQCD approach to be valid, a very encouraging

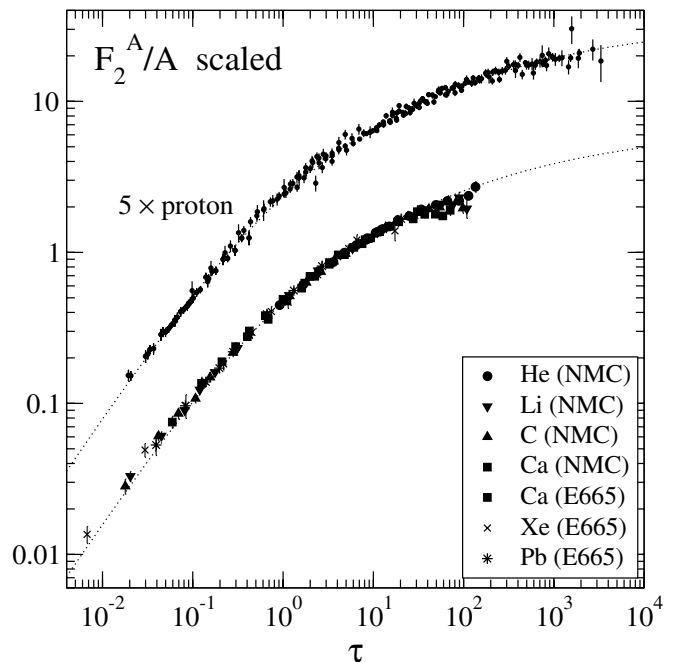


FIG. 3. Scaling behavior of NMC and E665  $F_2^A$  data vs  $\tau = \frac{(x_{bj})^{2\lambda} Q^2}{A^{1/\lambda}}$ . The vertical axis corresponds to the left-hand side of Eq. (5). The dashed line corresponds to the geometric scaling curve obtained from HERA data. These are shown offset by a factor of 5.

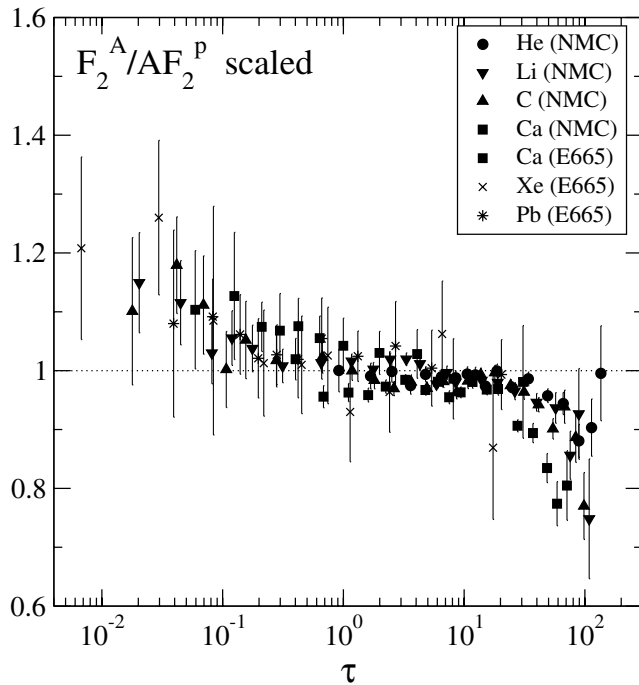


FIG. 4. Plot of scaled NMC and E665  $F_2^A/AF_2^P$  data vs  $\tau = \left(\frac{x_{bj}}{x_0}\right)^{2\lambda} \frac{Q^2}{A^{1/3}}$ . This corresponds to “dividing the data shown in Fig. 3 by the dashed line.”

sign, indeed. To contrast the scaling behavior we have included data points above  $\tau = 20$  which fall well into the antishadowing region and below  $\tau = 0.1$  which have  $Q^2$  values deeply in the nonperturbative domain. Also note that there is a consistent difference in the E665 and NMC data with the E665 data being much flatter in the ratio  $2F_2^A/AF_2^D$ , as evidenced in the comparison between the two calcium data sets and shown in Fig. 4. This apparent inconsistency between the two data sets disappears when the ratio  $12F_2^A/AF_2^C$  is compared between the two experiments [21].

Notwithstanding all of the above, nuclear data from the proposed Electron Ion Collider at BNL on heavy nuclei at small  $x_{bj}$  and large  $Q^2$  is necessary to be absolutely definitive about geometric scaling in inclusive  $eA$  scattering. These experiments will by design provide data at smaller  $x_{bj}$ , but one should take care to open up the phase space region. Only if we have access to a range of  $x_{bj}$  values at any given  $Q^2$  (and vice versa) for each species  $A$  can we obtain independent fits for the evolution rate  $\lambda$ . This would be a prerequisite to experimentally disentangle and confirm the  $A$  and  $x_{bj}$  dependence extracted simultaneously above. As the errors on the nuclear data get smaller one would also require a direct measurement of  $F_2^A/AF_2^D$  that would allow us to do away with our rather cavalier treatment of  $F_2^D/2F_2^P$ .

*Conclusions.*—To summarize, we demonstrate for the first time that the NMC and E665 data for the nuclear

structure function  $\frac{1}{A}F_2^A$  also exhibit geometric scaling as already seen in the nucleon structure function  $F_2^P$ . This has been confirmed by extrapolation of Eq. (4), which is valid at  $b = 0$ , small  $x_{bj}$ , and large enough  $Q^2$  and  $A$ , to presently available nuclear data. As these are at rather low  $Q^2$  and large  $x_{bj}$ , we had to allow slight modifications in the powers entering the  $A$  dependence in order to get a perfect fit. The NMC data for calcium, the heaviest nucleus available within this data set, would in fact be compatible with the  $A^{1/3}$  scaling. Given the limited phase space regions covered in the data sets we find it very encouraging how well the geometric scaling in  $eA$  follows the one in  $ep$ .

A. F. was supported by the DFG Emmy-Noether Grant, A. S. by BMBF, and H. W. by the DFG Habilitanden-program.

- 
- [1] L. D. McLerran and R. Venugopalan, Phys. Rev. D **49**, 2233 (1994),
  - [2] L. D. McLerran and R. Venugopalan, Phys. Rev. D **49**, 3352 (1994),
  - [3] J. Jalilian-Marian, A. Kovner, L. D. McLerran, and H. Weigert, Phys. Rev. D **55**, 5414 (1997).
  - [4] I. Balitsky, Nucl. Phys. **B463**, 99 (1996).
  - [5] J. Jalilian-Marian, A. Kovner, A. Leonidov, and H. Weigert, Phys. Rev. D **59**, 014014 (1999).
  - [6] J. Jalilian-Marian, A. Kovner, and H. Weigert, Phys. Rev. D **59**, 014015 (1999).
  - [7] Y. V. Kovchegov, Phys. Rev. D **60**, 034008 (1999).
  - [8] H. Weigert, Nucl. Phys. **A703**, 823 (2002).
  - [9] E. Iancu, A. Leonidov, and L. D. McLerran, Nucl. Phys. **A692**, 583 (2001).
  - [10] E. Ferreira, E. Iancu, A. Leonidov, and L. McLerran, Nucl. Phys. **A703**, 489–538 (2002).
  - [11] K. Golec-Biernat and M. Wusthoff, Phys. Rev. D **59**, 014017 (1999).
  - [12] H1 Collaboration, I. Abt *et al.*, Nucl. Phys. **B407**, 515 (1993).
  - [13] ZEUS Collaboration, M. Derrick *et al.*, Phys. Lett. B **316**, 412 (1993).
  - [14] A. M. Stasto, K. Golec-Biernat, and J. Kwiecinski, Phys. Rev. Lett. **86**, 596 (2001).
  - [15] J. Jalilian-Marian, A. Kovner, A. Leonidov, and H. Weigert, Nucl. Phys. **B504**, 415 (1997).
  - [16] K. Rummukainen and H. Weigert (to be published).
  - [17] New Muon Collaboration, M. Arneodo *et al.*, Nucl. Phys. **B487**, 3 (1997).
  - [18] E665 Collaboration, M. R. Adams *et al.*, Z. Phys. C **65**, 225 (1995).
  - [19] E665 Collaboration, M. R. Adams *et al.*, Z. Phys. C **67**, 403 (1995).
  - [20] HERMES Collaboration, A. Airapetian, hep-ex/0210068.
  - [21] NMC Collaboration (private communication).